

Effect of the electrical double layer on the electrical conductivity of suspensions

M. Ya. Sushko¹ and S. D. Balika

Department of Theoretical Physics and Astronomy, Mechnikov National University, 2 Dvoryanska St., Odesa 65026, Ukraine

Keywords: suspension, electrical double layer, stagnant layer, electrical conductivity, zeta-potential

Abstract

We study the role of the electrical double layer (EDL) in the formation of the quasistatic electrical conductivity of suspensions of nanosized particles. A suspension is viewed as a system of hard-core–penetrable-shell particles. The shells are electrically inhomogeneous, with a radially symmetrical conductivity profile. It is assumed that the real microstructure of the suspension can be reflected in terms of this profile and also the rule of dominance for overlapping regions that the local conductivity in the system is determined by the nearest particle. Using our earlier rigorous results for systems with this morphology, we derive general integral relations for the desired conductivity which incorporate the effect of the EDL and make it possible to look into the contributions from its different parts and parameters. Specific features, internal consistency, and flexibility of the model are demonstrated by further elaborating it to describe experimental data for latex suspensions in aqueous electrolyte solutions with high ionic strength.

1. Introduction

Development of new materials that, on the one hand, possess desired and controllable electrophysical properties and, on the other, are relatively cheap to manufacture requires reliable theoretical methods for evaluation of their relevant characteristics. Random heterogeneous materials (like composite solid electrolytes [1–4], composite polymeric electrolytes [5, 6], or suspensions in electrolyte solutions [7]) represent a class of systems that are already in wide use, but whose effective parameters (the effective electrical conductivity σ_{eff} among those) are very difficult to analyze theoretically. Two of the challenging issues in doing so are: (a) modeling of the microstructure of the system, with consideration for the presence of interface regions and possible variations of the microstructure with the volume concentration c of the filler; and (b) electrodynamic homogenization (finding σ_{eff}) of the proposed model, with taking into account many-particle effects.

This work presents a many-particle approach designed to quantitatively describe the effect of the electrical double layer (EDL) on the quasistatic σ_{eff} of suspensions. The EDL is a spatial distribution of ions that forms near a charged particle-base liquid interface. Its structure is rather complex [8, 9], but for our purposes can be considered as consisting of two major parts (see figure 1):

1. The inner part that comprises the Stern layer (with thickness of order of the ionic radius) and the stagnant layer (which is the starting part of the diffuse EDL). The electric potential at the boundary between these layers is called the diffuse-layer or Stern potential, ψ .
2. The outer part that is the remaining part of the diffuse EDL.

The two parts of the EDL are separated by the slip plane (at a distance d^* from the interface) the potential at which is the zeta-potential, ζ . In contrast to ψ , ζ is considered as a rather well-defined quantity obtainable from electrophoretic measurements.

The stagnant layer is believed to be hydrodynamically immobile, but, possibly, electrically conductive. The conductivity of the outer part is formed by hydrodynamically mobile ions moving under the electric

¹Corresponding author. E-mail: mrs@onu.edu.ua

field in the bulk of the carrying liquid. Because of thermal motion of ions, the slip plane between them is in reality partly spread, not sharp.

Standard electrokinetic theories [10–13] disregard the presence of the stagnant layer. They reduce the problem of finding σ_{eff} to an analysis of a system of coupled nonlinear differential equations and relations for the flow field and quantities related to the ion and electric potential distributions around a single particle. However, if the particle is viewed as a uniform hard sphere (of radius a), the system of the governing equations (including the Poisson-Boltzmann equation) is written for the exterior of the sphere, and the boundary conditions at the particle’s surface are those for the hard sphere, then systematic discrepancies occur between the values of ζ obtained from electrophoretic mobility and conductivity calculations [14]. These discrepancies are explained by a transport of ions within the Stern layer [15–17]. Analysis [18, 19] of the modifications in the Stern-layer transport theory for two mechanisms of Stern-layer adsorption of ions (onto available surface area and onto underlying surface charge) and the resulting boundary conditions shows that, regardless of the mechanism, the presence of mobile Stern-layer ions causes the electrophoretic mobility to decrease and the electrical conductivity to increase, as compared to the case when surface conduction is absent. The same conclusion is drawn from a cell model [20] for concentrated suspensions with hydrodynamic and electric interactions between particles.

It is important to emphasize that according to its original definition, surface conductance is the excess conduction within the slip plane; in general, it incorporates the effects from the stagnant layer [21], in addition to those from the Stern-layer. Now that the existence of a hydrodynamically stagnant layer is confirmed by molecular dynamic simulations [8], attempts are necessary to investigate its role in the formation of electrokinetic parameters and correctly interpret experimental data. One such an attempt [22, 23], free of in-depth detailing the structure of the stagnant layer, represents an extension of the thin-double-layer theory [24, 25] for dilute sols of spherical particles.

Incorporating the stagnant layer (or an analogue of it) into the model for σ_{eff} seems very promising. In what follows, we suggest that the factors behind the behavior of σ_{eff} with c can be illustrated by this schematic picture:

1. The effective conductivity σ_{eff} at low c is first of all a result of formation of conducting paths in the bulk of the suspension. These paths are formed by the mobile ions beyond the slip plane, that is, the outer part of the diffuse EDL.
2. The potential ζ at and the conductivity distribution within the slip plane result from the surface conduction processes occurring within the inner part of the EDL at a given κa (κ^{-1} is the Debye length).
3. The location of the slip plane is controlled by the thickness d^* of the inner part of the EDL. In view of an ionic-size thickness of the Stern layer, this is actually the thickness of the stagnant layer (or an analogue of it).
4. The properties of the stagnant layer are system-dependent. As a result, even for suspensions with equal ζ and κa , σ_{eff} is not a universal function of c , but also depends on the relative thickness $u^* = d^*/a$ of the inner part of the EDL. Data obtained by several electrokinetic techniques must be available to reliably estimate the governing parameters.
5. For given ζ , κa , and u^* , σ_{eff} changes in response to transformations of the system of conducting paths in the bulk, which include (at sufficiently high c) overlappings of the outer parts of the EDLs. The values of c at which the inner parts of the EDLs start overlapping are hardly achievable for real suspensions.

Viewing a suspension as a system of hard-core–penetrable-shell particles [26], generalizing this model to the case of inhomogeneous shells [27, 28], and using the compact-group approach [29, 30] for electrodynamic homogenization, we can integrate these factors and their effects into a single model to derive and analyze rigorous integral relations for σ_{eff} of suspensions with different conductive properties of the stagnant layer.

The subsequent presentation of our results is organized as follows. The basics of the core-shell model and compact-group approach are outlined in section 2. The elaboration of the model for suspensions and the derivation of the indicated relations for σ_{eff} are given in section 3. Applications of the theory to real

electrolyte-based suspensions are discussed in section 4. The major results of the work are summarized in section 5.

2. Model and method for finding σ_{eff}

Describing the model under consideration and the method for its homogenization, we omit numerous technical details and justifications; the interested reader will find them in the above mentioned articles [26–30] by the authors.

2.1. Microstructure of the model system

We assume that the electrical properties of a real suspension are equivalent to those of a model system that is made up by embedding hard-core-penetrable-shell particles into a fictitious uniform matrix with a complex permittivity $\hat{\epsilon}_f$ (see figure 1). The particles are considered to be stationary. This is a typical approximation in electrical conductivity problems, if the particles are sufficiently massive and alternating probing fields (of even low frequencies) are used. Experimentally its validity is controlled by varying the measurement frequency to make sure that the measurement results are independent of it. The microstructure of this model system is described in terms of the low-frequency complex permittivity distributions for its constituents. Each core is a uniform hard sphere of radius a and complex permittivity $\hat{\epsilon}_1$; it is associated with a real particle. Each shell is isotropic, but electrically inhomogeneous in the radial direction. Its complex permittivity profile is a piecewise continuous function $\hat{\epsilon}_2 = \hat{\epsilon}_2(r)$ that approaches the complex permittivity $\hat{\epsilon}_0$ of the base liquid as $r \rightarrow \infty$, r being the distance from the center of the sphere to the point of interest. The explicit expression for $\hat{\epsilon}_2(r)$ is modeled so as to account for different mechanisms contributing to the electrical characteristics of the real suspension at different values of c . For this purpose, the theory is complemented by a rule of dominance imposed on the electrical properties of overlapping regions which states: (a) the electrical properties of hard cores dominate over those of the shells and (b) those of closer (to the surface of a given core) parts of the shells over those of farther parts. This rule is necessary to define the electrical microstructure of the suspension uniquely, with consideration for its variations with c (see [27, 28]). Physically, this rule means that the local value of the complex permittivity in the system is determined by the distance from the point of interest to the closest particle. The outermost part of $\hat{\epsilon}_2(r)$ accounts for the electrical properties of the suspending liquid and its contribution to σ_{eff} .

2.2. Basics of the compact group approach

The quasistatic response of the model system to probing radiation is analyzed using the notion of compact groups of inhomogeneities. These groups are defined as macroscopic regions that are much smaller than the wavelength λ of the probing field in the medium, yet large enough to retain the properties of the entire system. The model system is viewed as a collection of such regions, with the complex permittivity distribution in it given by

$$\hat{\epsilon}(\mathbf{r}) = \hat{\epsilon}_f + \delta\hat{\epsilon}(\mathbf{r}), \quad (1)$$

where $\delta\hat{\epsilon}(\mathbf{r})$ is the contribution from the compact group located at point \mathbf{r} and comprising both particles and the base liquid. Since compact groups are point-like with respect to λ , their contributions to the average complex electric field $\langle \mathbf{E} \rangle$ and average complex electric current $\langle \mathbf{J} \rangle$ are formed by those values of the coordinates where the inner propagators in the corresponding iterative series reveal singular behavior. Moreover, for a macroscopically isotropic and homogeneous system it is only the δ -function singularities in these propagators that give non-zero contributions to $\langle \mathbf{E} \rangle$ and $\langle \mathbf{J} \rangle$. This fact allows us to single out the compact group contributions from the iterative series to express $\langle \mathbf{E} \rangle$ and $\langle \mathbf{J} \rangle$ in terms of the moments of $\delta\hat{\epsilon}(\mathbf{r})$ without employing any specific assumptions about multiple reemissions and many-particle correlations inside compact groups:

$$\langle \mathbf{E} \rangle = \left[1 + \sum_{s=1}^{\infty} \left(-\frac{1}{3\hat{\epsilon}_f} \right)^s \langle (\delta\hat{\epsilon}(\mathbf{r}))^s \rangle \right] \mathbf{E}_0, \quad (2)$$

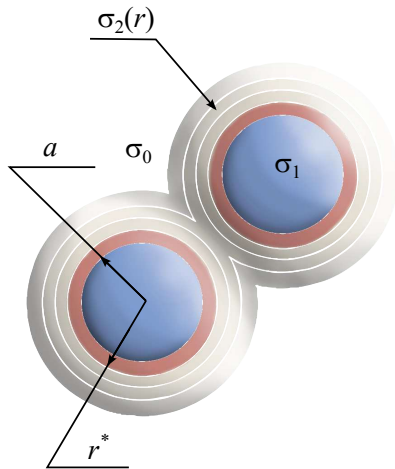


Fig. 1: Hard-core-penetrable-shell particles under consideration. Each shell consists of two concentric parts, separated by a spherical surface of radius r^* (at relative distance $u^* = (r^* - a)/a$ from the core). The inner and outer shells are associated with the inner and outer parts of the EDL, and the separating surface is associated with the slip plane at ζ -potential. The radius of the outer shell, shown as finite for illustrative purposes, is taken to tend to infinity in the final formula. The complex permittivity of each constituent [including the fictitious matrix ($\hat{\epsilon}_f$) and the homogenized system ($\hat{\epsilon}_{\text{eff}}$), both not shown] is taken in the form $\hat{\epsilon} = \epsilon + i\sigma/e_0\omega$, where ϵ and σ are respectively the quasistatic dielectric constant and electrical conductivity of the constituent, ω is the angular frequency of probing radiation, e_0 is the electric constant, and i is the imaginary unit. The resulting relation for σ_{eff} involves the conductivities σ_1 , $\sigma_2(r)$, and σ_0 of the core, shell, and base liquid, respectively. The variable $u = (r - a)/a$ defines the relative distance from the surface of the core to the point of interest.

$$\langle \mathbf{J} \rangle = -i\omega e_0 \hat{\epsilon}_f \left[1 - 2 \sum_{s=1}^{\infty} \left(-\frac{1}{3\hat{\epsilon}_f} \right)^s \langle (\delta\hat{\epsilon}(\mathbf{r}))^s \rangle \right] \mathbf{E}_0, \quad (3)$$

where \mathbf{E}_0 is the amplitude of the probing field in the fictitious matrix. The effective permittivity $\hat{\epsilon}_{\text{eff}}$ is defined as the proportionality coefficient in the relation

$$\langle \mathbf{J}(\mathbf{r}) \rangle = -i\omega e_0 \langle \hat{\epsilon}(\mathbf{r}) \mathbf{E}(\mathbf{r}) \rangle = -i\omega e_0 \hat{\epsilon}_{\text{eff}} \langle \mathbf{E}(\mathbf{r}) \rangle. \quad (4)$$

In his pioneering work [31], Maxwell calculated the effective electrical conductivity for a system of uniform hard spheres by comparing the large-distance asymptotic expressions for the electric potentials produced by a single such a sphere and a large sphere composed of many such spheres, assuming no electromagnetic interaction among them. The compact group approach is actually a rigorous and technically-different implementation of this idea by using the multiple scattering and generalized function theories for a system of particles whose electromagnetic interactions lead to the formation of the mean electric field (2) in the system. The moments $\langle (\delta\hat{\epsilon}(\mathbf{r}))^s \rangle$, $s \geq 1$, of $\delta\hat{\epsilon}(\mathbf{r})$ account for the effects of reemissions of order s within compact groups ('large spheres'). Maxwell's formula is obtained from (2) and (3) under the conditions that the particles are hard, $\hat{\epsilon}_f = \hat{\epsilon}_0$, and $\omega \rightarrow 0$.

The concept of the homogenized medium for a given system is physically meaningful if (a) the values of $\hat{\epsilon}_{\text{eff}}$ obtainable by using different operational definitions for $\hat{\epsilon}_{\text{eff}}$ are the same, and (b) the standard boundary conditions of electrodynamics remain valid for all constituents of the system and the homogenized medium as well. The compact group approach is compatible with these requirements if

$$\hat{\epsilon}_f = \hat{\epsilon}_{\text{eff}}. \quad (5)$$

In other words, it is an internally-closed homogenization procedure of the Bruggeman type.

In view of (2)–(5), the equation for $\hat{\varepsilon}_{\text{eff}}$ takes the form

$$\sum_{s=1}^{\infty} \left(-\frac{1}{3\hat{\varepsilon}_f} \right)^s \langle (\delta\hat{\varepsilon}(\mathbf{r}))^s \rangle = 0. \quad (6)$$

The equation for σ_{eff} is obtained by passing to the static limit $\omega \rightarrow 0$ in this relation.

2.3. General relation for σ_{eff} of the model system

Equation (6) holds regardless of the specific form of the expression for $\delta\hat{\varepsilon}(\mathbf{r})$. To advance, this expression must be constructed now for the model system. Using the indicator (or characteristic) function, defined for a region Ω as

$$\Pi_{\Omega}(\mathbf{r}) = \begin{cases} 1 & \text{if } \mathbf{r} \in \Omega \\ 0 & \text{if } \mathbf{r} \notin \Omega \end{cases}$$

this can be done as follows.

Partitioning each shell into very thin concentric spherical layers with outer radii r_j ($> a \equiv r_0$) and complex permittivities $\hat{\varepsilon}_{2,j}$, we can write down $\delta\hat{\varepsilon}(\mathbf{r})$ as

$$\delta\hat{\varepsilon}(\mathbf{r}) = (\hat{\varepsilon}_1 - \hat{\varepsilon}_{\text{eff}}) \Pi_1(\mathbf{r}) + \sum_{j \geq 1} (\hat{\varepsilon}_{2,j} - \hat{\varepsilon}_{\text{eff}}) \tilde{\Pi}_{2,j}(\mathbf{r}), \quad (7)$$

where $\tilde{\Pi}_{2,j}(\mathbf{r}) = \Pi_{2,j}(\mathbf{r}) - \Pi_{2,j-1}(\mathbf{r})$, with $\Pi_{2,j}(\mathbf{r})$ ($\Pi_{2,0}(\mathbf{r}) \equiv \Pi_1(\mathbf{r})$) being the characteristic functions of the subsystems of balls of radii r_j . Then, due to the properties of characteristic functions and the orthogonality of any two functions from the set $\{\Pi_1, \tilde{\Pi}_{2,j}\}$, we find

$$\langle (\delta\hat{\varepsilon}(\mathbf{r}))^s \rangle = c (\hat{\varepsilon}_1 - \hat{\varepsilon}_{\text{eff}})^s + \sum_{j \geq 1} [\phi(c, u_j) - \phi(c, u_{j-1})] (\hat{\varepsilon}_{2,j} - \hat{\varepsilon}_{\text{eff}})^s, \quad (8)$$

where $\phi(c, u_j) = \langle \Pi_{2,j}(\mathbf{r}) \rangle$ is the volume concentration of hard-core-penetrable-shell particles whose shells have relative thickness u_j . Estimates for $\phi(c, u)$ are obtained by statistical physics calculations (see, for instance, [32, 33]).

Passing in the moments (8) to integration, substituting them into (6), carrying out the summation, and, finally, passing to the static limit, we obtain the general equation for σ_{eff} :

$$c \frac{\sigma_1 - \sigma_{\text{eff}}}{2\sigma_{\text{eff}} + \sigma_1} + \int_0^{\infty} \frac{\partial \phi(c, u)}{\partial u} \frac{\sigma_2(u) - \sigma_{\text{eff}}}{2\sigma_{\text{eff}} + \sigma_2(u)} du = 0. \quad (9)$$

This equation is rigorous in the static limit and serves as the starting point for further analysis of suspensions. In the case of finite-thickness shells, it reproduces our earlier equation [28] which has proven to be efficient in describing composite solid and composite polymeric electrolytes.

3. Elaboration of the model for suspensions

Equation (9) is quite general. Now, we intend to add more details to the model to account for specific features of the EDL and the effects of its different parts on σ_{eff} of suspensions. In doing so, we focus on the situations where the number of fitting parameters in the model can be reduced to the least possible.

3.1. Accounting for the Stern layer

As was indicated, ion transport in the Stern layer can change the conductivity of the particle. Taking into account that the thickness of this layer is comparable with the ion size and, macroscopically, it is located at $u = 0$, we suggest that this effect can be incorporated into the theory by redefining σ_1 to be the conductivity that the particle has in the suspension, not before being embedded into it. Similar alteration of the conductive properties of constituents in the course of combining them into a system is observed, for instance, in composite polymeric electrolytes [27].

The other effects of the Stern layer—on the adjacent stagnant layer and the potential distribution near the particle—are actually incorporated via the parameters (conductivity and thickness) of the stagnant layer and ζ -potential, as discussed below.

3.2. Accounting for the stagnant layer

Due to a specific structure of the integrand, three particular situations can be analyzed in-depth based only on very general assumptions about the behavior of $\sigma_2(u)$ in the stagnant layer, by which the inner part $u \in (0, u^*)$ of the diffuse EDL is meant:

1. *Highly-conductive stagnant layer:* $\sigma_2(u) \gg \sigma_{\text{eff}}$ for $u \in (0, u^*)$.

In this case, splitting the integral in (9) into one over the region $u \in (0, u^*)$ and the other over the region $u \in (u^*, \infty)$ gives

$$c \frac{\sigma_1 - \sigma_{\text{eff}}}{2\sigma_{\text{eff}} + \sigma_1} + F(c, u^*) + \int_{u^*}^{\infty} \frac{\partial \phi(c, u)}{\partial u} \frac{\sigma_2(u) - \sigma_{\text{eff}}}{2\sigma_{\text{eff}} + \sigma_2(u)} du = 0, \quad (10)$$

where

$$F(c, u^*) = \int_0^{u^*} \frac{\partial \phi(c, u)}{\partial u} du = \phi(c, u^*) - c,$$

for $\phi(c, 0) = c$. Then, resolving the fraction in the integrand into partial fractions, adding and subtracting the term

$$3\sigma_{\text{eff}} \int_{u^*}^{\infty} \frac{\partial \phi(c, u)}{\partial u} \frac{1}{2\sigma_{\text{eff}} + \sigma_0} du,$$

and taking into account that

$$\int_{u^*}^{\infty} \frac{\partial \phi(c, u)}{\partial u} du = 1 - \phi(c, u^*),$$

we obtain

$$\begin{aligned} & [1 - \phi(c, u^*)] \frac{\sigma_0 - \sigma_{\text{eff}}}{2\sigma_{\text{eff}} + \sigma_0} + c \frac{\sigma_1 - \sigma_{\text{eff}}}{2\sigma_{\text{eff}} + \sigma_1} + F(c, u^*) \\ & - 3\sigma_{\text{eff}} \int_{u^*}^{\infty} \frac{\partial \phi(c, u)}{\partial u} \left[\frac{1}{2\sigma_{\text{eff}} + \sigma_2(u)} - \frac{1}{2\sigma_{\text{eff}} + \sigma_0} \right] du = 0. \end{aligned} \quad (11)$$

In particular, for nonconducting particles ($\sigma_1 \rightarrow 0$) (11) reduces to

$$[1 - \phi(c, u^*)] \frac{\sigma_0 - \sigma_{\text{eff}}}{2\sigma_{\text{eff}} + \sigma_0} + F_0(c, u^*) - 3\sigma_{\text{eff}} \int_{u^*}^{\infty} \frac{\partial \phi(c, u)}{\partial u} \left[\frac{1}{2\sigma_{\text{eff}} + \sigma_2(u)} - \frac{1}{2\sigma_{\text{eff}} + \sigma_0} \right] du = 0 \quad (12)$$

with

$$F_0(c, u^*) = \phi(c, u^*) - \frac{3}{2}c. \quad (13)$$

2. *Low-conductive stagnant layer:* $\sigma_2(u) \ll \sigma_{\text{eff}}$ for $u \in (0, u^*)$.

Proceeding in the same way, we arrive at (11) and (12) again, but with

$$F(c, u^*) = -\frac{1}{2}[\phi(c, u^*) - c], \quad F_0(c, u^*) = -\frac{1}{2}\phi(c, u^*). \quad (14)$$

3. *Conductivity of the stagnant layer is comparable with the effective one:* $\sigma_2(u) \approx \sigma_{\text{eff}}$ for $u \in (0, u^*)$.

Now, assuming the contribution from the integral over $u \in (0, u^*)$ to be negligible as compared to that over $u > u^*$, we have (11) and (12) with

$$F = 0, \quad F_0(c) = -\frac{1}{2}c. \quad (15)$$

Note that the physical meaning of each addend in (11) is clear. The first one is the contribution from the base liquid. The second one describes the contribution from the particles whose conductivities incorporate the effect of ionic transport in the Stern layer. The third one is the contribution from the inner part of the diffuse EDL. And the fourth one describes the effect of the outer part of the diffuse EDL. Of course, all these contributions are interrelated.

3.3. Accounting for the outer part of the EDL

Beyond the slip plane, the conductivity is formed by mobile ions in the diffuse EDL. Let z_a , μ_a , and n_a be respectively the charge numbers, mobilities, and average number densities of the ions in the carrying liquid. Assuming the Boltzmann distribution to be valid for the region $u > u^*$ about a given particle, we model the one-particle profile $\sigma_2(u)$ for $u > u^*$ as

$$\sigma_2(u) = e \sum_a |z_a| \mu_a n_a e^{-z_a y(u)}, \quad (16)$$

where $y(u) = e\varphi(u)/k_B T$, $\varphi(u)$ is the electric potential distribution for $u > u^*$, such that $\varphi(u^*) = \zeta$, k_B is the Boltzmann constant, T is the temperature, and e is the elementary charge. Neither u^* nor $y(u)$ is supposed to be extrapolated to the surface of the particle. In general, $y(u)$ is unknown—since it depends on the locations of the other particles as well, finding it for arbitrary c is a challenging many-particle problem. Yet in situations where the overlapping of the EDLs can be ignored, we expect well-known one-particle solutions to be applicable for $y(u)$.

4. Application to electrolyte-based suspensions

To put our model to the test and elucidate the role that the diffuse EDL can play in the formation of σ_{eff} , we consider here a suspension of nonconducting particles in an aqueous 1:1 electrolyte solution with high ionic strength. Extensive experimental data for σ_{eff} of such suspensions are given in [14]. In order to reduce the number of fitting parameters to the least number possible, we also assume that (a) the effect of the Stern layer on the conductivity of the particles is negligible, so $\sigma_1 = 0$; and (b) the ion mobilities in

the EDL beyond the slip plane are equal to those in the bulk of the suspending liquid. It turns out that under these assumptions, experimental data [14] can be recovered using only a single fitting parameter, the relative thickness u^* of the stagnant layer.

The models with an adjustable σ_1 and the ion mobilities whose values near the surfaces of particles (say, due to the convective contribution [34]) and those in the bulk are in general different are, of course, more flexible and include the case under consideration. They are also encompassed by our general formalism. The study of them is a matter for further analysis which, however, goes beyond the scope of this work.

4.1. Working equations

The fact that $\kappa a \gg 1$ means that, first, overlapping of the EDLs is negligible up to rather high c ; and, second, the curvature of the EDL is very small, which implies that the Gouy-Chapman solution for planar surfaces can be used to describe the radial distribution of the electric potential in the EDL beyond the slip plane:

$$y(u) = 2 \ln \left[\frac{1 + \gamma e^{-\kappa a(u-u^*)}}{1 - \gamma e^{-\kappa a(u-u^*)}} \right], \quad \gamma = \tanh \left(\frac{y\zeta}{4} \right), \quad y\zeta = \frac{e\zeta}{k_B T}. \quad (17)$$

The corresponding distribution of the electrical conductivity is

$$\sigma_2(u) = e\mu_+ n_0 e^{-y(u)} + e\mu_- n_0 e^{y(u)}, \quad u > u^*, \quad (18)$$

where μ_+ and μ_- are respectively the cation and anion mobilities (assumed to be independent of the electric field), and n_0 is the average number density of ions of each type. As $u \rightarrow \infty$, $\sigma_2(u)$ tends to $\sigma_0 = e\mu_+ n_0 + e\mu_- n_0$, the conductivity of the carrying liquid.

Denote $m \equiv \mu_+/\mu_-$. Simple analysis reveals that provided (a) $m > 1$ for $\zeta > 0$ or (b) $0 < m < 1$ for $\zeta < 0$, there are intervals of u where $\sigma_2(u) < \sigma_0$ (see figure 2). The volume fraction of such regions increases as c is increased, which can cause σ_{eff} to decrease even in the case of highly conductive stagnant layers. On the other hand, the condition $\sigma_2(u) > \sigma_0$ does not assure that σ_{eff} is an increasing function of c .

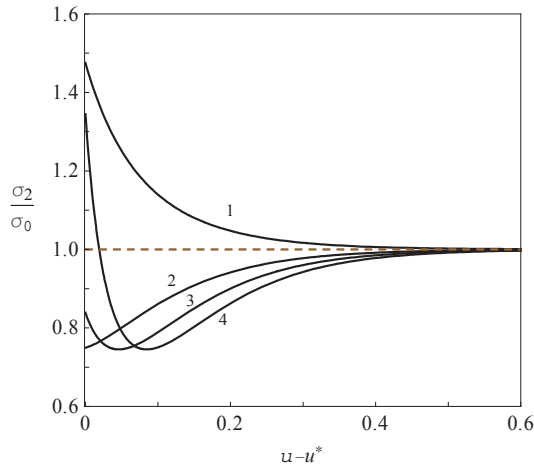


Fig. 2: Normalized conductivity $x_2(u) = \sigma_2(u)/\sigma_0$ as a function of $u - u^*$ for $u \geq u^*$, according to (17) and (18) at $\kappa a = 10$, $m = 5$, and $y\zeta = -0.5, 0.7, 1.3$, and 2 (curves 1 to 4, respectively). The plots for $0 < m < 1$ and the opposite values of $y\zeta$ look similar. The local minimum $x_2(u_0) = 2m^{1/2}/(m+1) < 1$ at $u_0 = u^* + (\kappa a)^{-1} \ln |\gamma(m^{1/4} + 1)/(m^{1/4} - 1)|$ appears beyond the slip plane if $|\gamma| > |m^{1/4} - 1|/(m^{1/4} + 1)$.

In what follows, we change to the normalized conductivities $x_2(u) = \sigma_2(u)/\sigma_0$ and $x_{\text{eff}} = \sigma_{\text{eff}}/\sigma_0$. According to (12) and (13), the suspension conductivity increment $\sigma_0^{-1} \partial \sigma_{\text{eff}} / \partial c$ ($c \rightarrow 0$), that is, the

normalized rate of change of σ_{eff} with respect to c for a diluted suspension, is given (in the case of highly conductive stagnant layers) by

$$\frac{\partial x_{\text{eff}}}{\partial c} = 3(1 + u^*)^3 - \frac{9}{2} + 9 \int_{u^*}^{\infty} (1 + u)^2 \frac{x_2(u) - 1}{2 + x_2(u)} du. \quad (19)$$

Also, introduce the second radial moment of the deviation of the normalized conductivity distribution beyond the slip plane from the conductivity of the carrying liquid:

$$m_2(r^*) = \int_{r^*}^{\infty} r^2 [x_2(r) - 1] dr = a^3 \int_{u^*}^{\infty} (1 + u)^2 [x_2(u) - 1] du. \quad (20)$$

With the use of these two quantities, the behavior of σ_{eff} for the situations in figure 2 can be quantified as follows:

1. $x_2(u) < 1$ for $u > u^*$ (curves 2 and 3 in figure 2)

The conductivity σ_{eff} decreases, $\partial x_{\text{eff}}/\partial c < 0$, provided

$$\int_{u^*}^{\infty} (1 + u)^2 \frac{x_2(u) - 1}{2 + x_2(u)} du < \frac{1}{2} - \frac{1}{3}(1 + u^*)^3. \quad (21)$$

The integral is negative, so this inequality holds for u^* up to a value of $(3/2)^{1/3} - 1 \simeq 0.145$, at least. For greater values of u^* , a further system-dependent analysis is needed.

Note that since now

$$\int_{u^*}^{\infty} (1 + u)^2 \frac{x_2(u) - 1}{2 + x_2(u)} du \geq \frac{1}{2} \int_{u^*}^{\infty} (1 + u)^2 [x_2(u) - 1] du,$$

a necessary condition for σ_{eff} to decrease can be written as

$$\frac{m_2(r^*)}{a^3} < 1 - \frac{2}{3} \frac{r^{*3}}{a^3}. \quad (22)$$

Ignoring the existence of the diffuse EDL leads to the Maxwell-Garnett result

$$\frac{\partial x_{\text{eff}}}{\partial c} \xrightarrow{c \rightarrow 0} -\frac{3}{2}.$$

2. $x_2(u) > 1$ for $u > u^*$ (curve 1 in figure 2)

The conductivity σ_{eff} increases, $\partial x_{\text{eff}}/\partial c > 0$, if

$$\int_{u^*}^{\infty} (1 + u)^2 \frac{x_2(u) - 1}{2 + x_2(u)} du > \frac{1}{2} - \frac{1}{3}(1 + u^*)^3. \quad (23)$$

The integral is now positive, so the inequality definitely holds for $u^* > (3/2)^{1/3} - 1 \simeq 0.145$. This estimate agrees with our earlier result for a model suspension of hard-core particles surrounded by highly-conductive uniform penetrable shells [26]. For smaller values of u^* , an additional analysis is required.

In the case under consideration,

$$\int_{u^*}^{\infty} (1 + u)^2 \frac{x_2(u) - 1}{2 + x_2(u)} du \leq \frac{1}{3} \int_{u^*}^{\infty} (1 + u)^2 [x_2(u) - 1] du.$$

If σ_{eff} increases, then, in view of the two previous equations,

$$\frac{m_2(r^*)}{a^3} > \frac{3}{2} - \frac{r^{*3}}{a^3}. \quad (24)$$

Physically, (24) is a necessary condition for σ_{eff} to increase with c that is imposed on $m_2(r^*)$. The value of this moment can be increased by (a) increasing $|\zeta|$, (b) decreasing κa , or (c) combining both ways.

3. $x_2(u) > 1$ for $u \in (u^*, u^{**})$, but $x_2(u) < 1$ for $u > u^{**}$ (curve 4 in figure 2)

The conductivity σ_{eff} decreases if inequality (21) holds. Split the integral into one over (u^*, u^{**}) and the other over (u^{**}, ∞) , where u^{**} is the solution to the equation $x_2(u^{**}) = 1$. Since the latter integral is negative, omitting it gives a sufficient condition for σ_{eff} to decrease:

$$\int_{u^*}^{u^{**}} (1+u)^2 \frac{x_2(u) - 1}{2 + x_2(u)} du < \frac{1}{2} - \frac{1}{3}(1+u^*)^3. \quad (25)$$

For (17) and (18), $u^{**} = u^* + (\kappa a)^{-1} \ln |\gamma (m^{1/2} + 1)/(m^{1/2} - 1)|$.

To complete the model, we use the following estimate for $\phi(c, u)$ [32] in our calculations:

$$\begin{aligned} \phi(c, u) = & 1 - (1-c) \exp \left[-\frac{((1+u)^3 - 1)c}{1-c} \right] \exp \left\{ -\frac{3(1+u)^3 c^2}{2(1-c)^3} \right. \\ & \times \left. \left[2 - \frac{3}{1+u} + \frac{1}{(1+u)^3} - \left(\frac{3}{1+u} - \frac{6}{(1+u)^2} + \frac{3}{(1+u)^3} \right) c \right] \right\}. \end{aligned} \quad (26)$$

For diluted suspensions ($c \rightarrow 0$),

$$\phi(c, u) = 1 - \exp \left[-(1+u)^3 c \right] + O(c^2). \quad (27)$$

Combined together, (12)–(15), (17), (18), and (26) make up closed models that differ by the values of the conductivity of the stagnant layer. We are now in a position to contrast their results with experiment.

4.2. Comparison with experiment

Tables 1 and 2 and figs. 3 and 4 summarize the results of applying our model to well-known experimental data [14] for suspensions of spherical and nearly monodisperse Latex A ($a = 83$ nm) and Latex B ($a = 235$ nm) particles in aqueous HCl and KCl solutions. The particles were synthesized by two different techniques. The concentration c was varied by successive dilution of suspension samples. The samples were thermostatted to $25 \pm 0.05^\circ\text{C}$. Conductivity measurement results with a bridge method at 80 and 1000 Hz were independent of frequency. Measurements of the latex electrophoretic mobility were carried out 20–40 times for each salt concentration (molarity M) and were stable. The ζ -potentials (columns 3 in the tables) were determined using several electrokinetic models ([10, 12] and others). The conductivity data revealed that for $\kappa a > 6$, the σ_{eff} vs c plots could be considered linear up to c amounting to several hundredths. The corresponding conductivity increments (columns 4) were reported for all data. Several conductivity plots were presented for Latex A in HCl.

Table 1: Results of processing σ_{eff} vs c data [14] for suspensions of latex particles in aqueous HCl solutions

M	κa	y_ζ	$\frac{\partial x_{\text{eff}}}{\partial c}, \text{exp.}$	$\frac{\partial x_{\text{eff}}}{\partial c}, \text{calc.}$	u^*	$d^*, \text{in } \kappa^{-1}$	(24)	T/F
Latex A, $a = 83$ nm								
1×10^{-2}	26.9	-2.27	-0.31 ± 0.02	-0.31	0.094	2.53	$0.150 < 0.190$	T
5×10^{-3}	19.1	-2.33	0.60 ± 0.05	0.53	0.153	2.92	$0.249 > -0.033$	T
1×10^{-3}	8.5	-2.44	3.10 ± 0.01	3.10	0.278	2.36	$0.006 > -0.196$	T
5×10^{-4}	6.0	-2.17	3.57 ± 0.06	3.61	0.280	1.68	$0.967 > -0.597$	T
Latex B, $a = 235$ nm								
5×10^{-3}	54.6	-3.22	-0.85 ± 0.07	-0.85	0.052	2.84	$0.006 < 0.336$	T
1×10^{-3}	24.4	-3.40	-0.30 ± 0.15	-0.30	0.083	2.03	$0.008 < 0.230$	T
5×10^{-4}	17.3	-2.89	1.33 ± 0.08	1.33	0.202	3.49	$0.007 > -0.237$	T
1×10^{-4}	7.7	-2.28	2.36 ± 0.23	2.37	0.228	1.76	$0.004 > -0.352$	T

Since the values $\kappa a \gtrsim 6$ are expected to belong to the region of validity of the Gouy-Chapman solution (17), our model is applicable to process the above data. We proceed as follows:

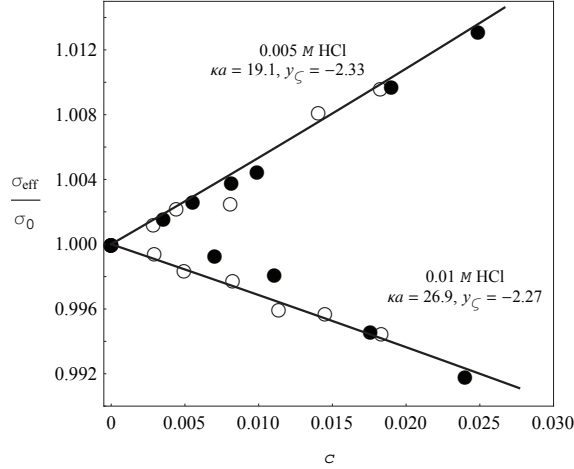


Fig. 3: σ_{eff} as a function of c for suspensions of Latex A particles in 1×10^{-2} and 5×10^{-3} M HCl; markers \bullet and \circ represent duplicate experiments starting from fresh latex [14]. Solid lines: our model results for reported κa and ζ and the fitting values of $u^* = 0.094$ ($d^* = 2.53 \kappa^{-1}$) and 0.153 ($d^* = 2.92 \kappa^{-1}$), respectively. The corresponding theoretical estimates (-0.31 and 0.53) and experimental data (-0.31 ± 0.02 and 0.60 ± 0.05) for $\partial x_{\text{eff}}/\partial c$ are in practical agreement. Condition (24) is not fulfilled and is fulfilled, respectively, as expected (see table 1).

1. Using given values of κa and ζ -potentials, and taking the ion mobilities to be $\mu_{\text{H}^+} = 36.29 \times 10^{-8} \text{ m}^2/\text{V}^{-1} \cdot \text{s}^{-1}$, $\mu_{\text{K}^+} = 7.6 \times 10^{-8} \text{ m}^2/\text{V}^{-1} \cdot \text{s}^{-1}$, and $\mu_{\text{Cl}^-} = 7.92 \times 10^{-8} \text{ m}^2/\text{V}^{-1} \cdot \text{s}^{-1}$, we find that the behavior of $x_2(u)$ for latex suspensions in HCl ($m = 4.58$) resembles that of curve 1 in fig. 2, and that for latex suspensions in KCl ($m = 0.96$) resembles that of curve 4.
2. Equating the theoretical expressions [(19) and its counterparts for the cases of stagnant layers with intermediate and low conductivities] and experimental data (columns 4) for the suspension conductivity increments, we calculate the values of u^* (columns 6) and then verify that they reproduce the reported increments within an experimental error (columns 5). The only slight exception is the value of u^* for Latex A suspensions in 5×10^{-3} M HCl, which is adjusted to fit the entire plot of σ_{eff} vs c available (see fig. 3). Nonetheless, the adjusted and reported values for $\partial x_{\text{eff}}/\partial c$ remain in practical agreement.

It must be emphasized that physically meaningful solutions for u^* occur only in the case of highly conductive stagnant layers.

3. Using the values of u^* obtained, we find that the slip plane in the suspensions under consideration is located near the edge (in the traditional physical meaning) of the diffuse EDL (columns 7). As the ionic strength of the electrolyte solutions decreases, this plane seems to have a tendency to penetrate deeper into the EDL. This can be explained by “softening” of the latter.
4. Finally, calculating the values of the left- and right-hand sides in (24) and (25), we make sure that in all cases, the directions of the resulting inequalities are in line with the expected ones (columns 8 and 9). This fact signifies the internal consistency of the proposed model.

So, our model, which employs a single fitting parameter u^* , is capable of describing σ_{eff} of the above suspensions of nanosized particles in a cohesive manner, the estimated values of u^* exhibiting similar trends. These processing results indicate that for the specified values of κa , y_ζ , and c , the electrical conductivity of the considered suspensions is contributed to by two factors: the presence of a highly conductive stagnant layer inside the slip plane and transport of mobile ions beyond it. Simple independent estimates in support of the existence of highly conductive interphase layers in nanofluids can also be found elsewhere [26].

It should also be remarked that rather considerable (in terms of the Debye length) values of u^* raise the question of accuracy of evaluating the ζ -potential of nanofluids with standard electrophoretic models; occurring inaccuracies may necessitate adjustments to the above results. A feasible approach to attacking this question may consist in a combined analysis of the results obtained with the proposed model for σ_{eff}

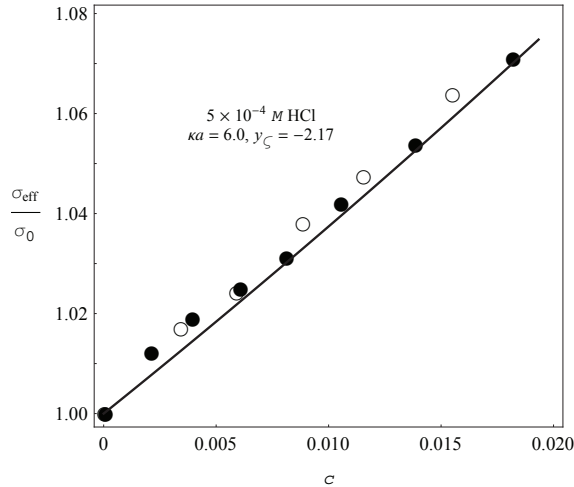


Fig. 4: σ_{eff} as a function of c for suspensions of Latex A particles in $5 \times 10^{-4} M$ HCl [14]. Solid line: our model results for reported κa and ζ and the fitting value of $u^* = 0.28$ ($d^* = 1.68 \kappa^{-1}$). The corresponding theoretical estimate $\partial x_{\text{eff}}/\partial c = 3.61$ is in agreement with experimental data 3.57 ± 0.06 . Condition (24) is fulfilled, as expected (see table 1).

and those with the method of laser correlation spectroscopy for the diffusion coefficient of nanoparticles in the nanofluid under study [35].

Table 2: Results of processing σ_{eff} vs c data [14] for suspensions of latex particles in aqueous KCl solutions

M	κa	y_ζ	$\frac{\partial x_{\text{eff}}}{\partial c}, \text{exp.}$	$\frac{\partial x_{\text{eff}}}{\partial c}, \text{calc.}$	u^*	$d^*, \text{in } \kappa^{-1}$	(25)	T/F
Latex A, $a = 83 \text{ nm}$								
1×10^{-2}	26.9	-3.06	-0.85 ± 0.05	-0.85	0.050	1.35	$0.018 < 0.114$	T
1×10^{-3}	8.5	-2.96	1.55 ± 0.08	1.55	0.209	1.78	$0.042 > -0.089$	T
Latex B, $a = 235 \text{ nm}$								
5×10^{-3}	54.6	-3.22	-0.57 ± 0.07	-0.58	0.082	4.48	$0.014 < 0.078$	T
1×10^{-3}	24.4	-3.40	0.00 ± 0.05	-0.005	0.120	2.93	$0.028 < 0.032$	T

5. Conclusion

Finding the electrical conductivity σ_{eff} of colloidal suspensions is a long-standing problem. It is typically studied by analyzing a system of coupled nonlinear equations and relations describing the ion transport in the vicinity of a single particle. Practical advances are possible after using a number of poorly controlled or uncontrolled approximations, employing model boundary conditions, and ignoring electromagnetic interactions between suspended particles. The individual roles of the parameters of the model are difficult to keep track of.

Considering a suspension as a system of particles with the hard-core-inhomogeneous-penetrable-shell morphology, we propose a new many-particle approach to the problem. As compared to previous publications in the field, its distinctive features are as follows: (1) it effectively incorporates both many-particle electromagnetic interactions among the structural units (particles, EDLs, and suspending liquid) of the suspension and variations of the system's microstructure as the concentration of the particles is changed; (2) the microstructure of the EDL is extended to include the stagnant layer (or an analogue of it) in between the Stern layer and the mobile diffuse part of the EDL; (3) under the assumptions of the model (modelling the microstructure of the system in terms of the electrical conductivity distributions in its structural units subject to certain rules of dominance for overlapping regions, and using our original method of compact

groups of inhomogeneities for electrodynamic homogenization), the quasistatic σ_{eff} is calculated rigorously without in-depth approximations typical of one-particle theories; (4) the rigorous integral relation obtained for σ_{eff} makes it possible to analyze individual roles of the parameters of the structural units (such as the ion concentrations and mobilities, slip plane location, ζ -potential, particle volume concentration, etc.) on σ_{eff} and to develop a system of inequalities for controlling the internal consistency of the model.

Specific features and efficiency of the model are demonstrated by elaborating and applying the general relation to the case of latex suspensions in aqueous electrolyte solutions with high ionic strength. A single fitting parameter, the relative thickness of the stagnant layer, proves to be sufficient to describe experiment.

The effect of the stagnant layer (the region in between the Stern layer and the slip plane) on σ_{eff} can remain significant in the systems where the mobile diffuse part of the EDL is suppressed. Based on our model, we demonstrated this fact recently [36] for concentrated suspensions of so-called ghost particles (fabricated by lysis from human erythrocytes) in aqueous NaCl and phosphate-buffered saline solutions of molarity 0.15.

Under certain conditions, both parts of the EDL can partially contribute to σ_{eff} of non-aqueous systems as well. For instance, the formation of an interface layer is reported based on the results of molecular dynamic simulation for Cu particles in liquid Ar [37] and calorimetric measurements for suspensions of Al_2O_3 particles in isopropyl alcohol [38]. On the other hand, the formation of the EDL-like layer around the particles can occur in such systems when the base liquid is slightly contaminated. Using an earlier version of the model under consideration, the effect of this layer on σ_{eff} was demonstrated in a specially-designed experiment for suspensions of Al_2O_3 in isopropyl alcohol [26]. It should be noted that in cases where the EDL is of little or no significance, our general formalism still applies and can be used to study, for instance, the properties of and the contribution to σ_{eff} from the suspending liquid [28].

The model allows for further diversification and can be considered as a flexible tool for analysis and design of electrical properties of suspensions.

References

- [1] Liang CC (1973) Conduction characteristics of the lithium Iodide-aluminum oxide solid electrolytes. *J Electrochem Soc* 120:1289-1292. <https://doi.org/10.1149/1.2403248>
- [2] Dudney NJ (1989) Composite electrolytes. *Annu Rev Mater Sci* 19:103-120. <https://doi.org/10.1146/annurev.ms.19.080189.000535>
- [3] Wagner JB (1989) Composite solid ion conductors. In: Takahashi T (ed) *Recent trends and applications*. World Scientific, Singapore, pp 146-165
- [4] Nan C-W (1993) Physics of inhomogeneous inorganic materials. *Prog Mater Sci* 37:1-116. [https://doi.org/10.1016/0079-6425\(93\)90004-5](https://doi.org/10.1016/0079-6425(93)90004-5)
- [5] Wiczcerek W, Sikierski M (2008) Composite polymeric electrolytes. In: Knauth P and Schoonman J (ed) *Nanocomposites. Ionic conducting materials and structural spectroscopies*. Springer, New York, pp 1-70
- [6] Sequeira C, Santos D (2010) *Polymer electrolytes. Fundamentals and applications*. Woodhead Publishing, Cambridge
- [7] Ohshima H (2012), *Electrical phenomena at Interfaces and biointerfaces. Fundamentals and applications*. In: Ohshima H (ed) *Nano-, bio-, and environmental sciences*, John Wiley & Sons, Hoboken, New Jersey
- [8] Lyklema J, Rovillard S, De Coninck J (1998) Electrokinetics: The properties of the stagnant layer unraveled. *Langmuir* 14(20):5659-5663. <https://doi.org/10.1021/la980399t>
- [9] Delgado AV, González-Caballero F, Hunter RJ, Koopal LK, Lyklema J (2005) Measurement and interpretation of electrokinetic phenomena (IUPAC technical report). *Pure Appl Chem* 77(10):1753-1805. <https://doi.org/10.1351/pac200577101753>
- [10] O'Brien RW and White LR (1978) Electrophoretic mobility of a spherical colloidal particle. *J Chem Soc Faraday Trans 2* 74:1607-1626 <https://doi.org/10.1039/F29787401607>
- [11] Saville DA (1979) Electrical conductivity of suspensions of charged particles in ionic solutions. *J Colloid Interface Sci* 71:477-490. [https://doi.org/10.1016/0021-9797\(79\)90322-9](https://doi.org/10.1016/0021-9797(79)90322-9)
- [12] O'Brien RW (1981) The electrical conductivity of a dilute suspension of charged particles. *J. Colloid Interface Sci* 81:234-248. [https://doi.org/10.1016/0021-9797\(81\)90319-2](https://doi.org/10.1016/0021-9797(81)90319-2)
- [13] DeLacey EHB, White LR (1981) Dielectric response and conductivity of dilute suspensions of colloidal particles. *J Chem Soc Faraday Trans 2* 77:2007-2039. <https://doi.org/10.1039/F29817702007>
- [14] Zukoski IV CF, Saville DA (1985) An experimental test of electrokinetic theory using measurements of electrophoretic mobility and electrical conductivity. *J Colloid Interface Sci* 107:322-333. [https://doi.org/10.1016/0021-9797\(85\)90184-5](https://doi.org/10.1016/0021-9797(85)90184-5)
- [15] Dukhin SS, Derjaguin BV (1974) *Electrokinetic phenomena. Surface and Colloid Science*, Wiley, New York, vol 7.
- [16] Zukoski IV CF, Saville DA (1986) The interpretation of electrokinetic measurements using a dynamic model of the Stern layer: I. The dynamic model. *J Colloid Interface Sci* 114(1):32-44. [https://doi.org/10.1016/0021-9797\(86\)90238-9](https://doi.org/10.1016/0021-9797(86)90238-9)
- [17] Zukoski IV CF, Saville DA (1986) The interpretation of electrokinetic measurements using a dynamic model of the Stern layer: II. Comparisons between theory and experiment. *J Colloid Interface Sci* 114(1):45-53. [https://doi.org/10.1016/0021-9797\(86\)90239-0](https://doi.org/10.1016/0021-9797(86)90239-0)

- [18] Mangelsdorf CS, White LR (1990) Effects of Stern-layer conductance on electrokinetic transport properties of colloidal particles. *J Chem Soc Faraday Trans* 86(16):2859-2870. <https://doi.org/10.1039/FT9908602859>
- [19] Mangelsdorf CS, White LR (1998) The dynamic double layer. Part 1 Theory of a mobile Stern layer. *J Chem Soc Faraday Trans* 94(16): 2441-2452. <https://doi.org/10.1039/A803588A>
- [20] Carrique F, Arroyo FJ, Delgado AV (2001) Electrokinetics of concentrated suspensions of spherical colloidal particles: Effect of a dynamic Stern layer on electrophoresis and DC conductivity. *J Colloid Interface Sci* 243(2): 351-361. <https://doi.org/10.1006/jcis.2001.7903>
- [21] Shilov VN, Dukhin SS (1970) Theory of polarization of a thin diffuse layer of spherical particle in alternating field. *Kolloidn. Zh.* 32:117-128.
- [22] Kijlstra J, van Leeuwen HP, Lyklema J (1992) Effects of surface conduction on the electrokinetic properties of colloids. *J Chem Soc Faraday Trans* 88(23):3441-3449 <https://doi.org/10.1039/FT9928803441>
- [23] Kijlstra J, van Leeuwen HP, Lyklema J (1993) Low-frequency dielectric relaxation of hematite and silica sols. *Langmuir* 9(7):1625-1633. <https://doi.org/10.1021/la00031a005>
- [24] Fixman M (1980) Charged macromolecules in external fields. I. The sphere *J Chem Phys* 72:5177-5186. <https://doi.org/10.1063/1.439753>
- [25] Fixman M (1983) Thin double layer approximation for electrophoresis and dielectric response. *J Chem Phys* 78:1483-1491. <https://doi.org/10.1063/1.444838>
- [26] Sushko MYa, Gotsulskiy VYa, Stiranets MV (2016) Finding the effective structure parameters for suspensions of nano-sized insulating particles from low-frequency impedance measurements. *J Mol Liq* 222:1051-1060. <https://doi.org/10.1016/j.molliq.2016.07.021>
- [27] Sushko MYa, Semenov AK (2019) A mesoscopic model for the effective electrical conductivity of composite polymeric electrolytes. *J Mol Liq* 279:677-686. <https://doi.org/10.1016/j.molliq.2019.02.009>
- [28] Sushko MYa, Semenov AK (2019) Rigorously solvable model for the electrical conductivity of dispersions of hard-core-penetrable-shell particles and its applications. *Phys Rev E* 100(5): 052601(14 pages). <https://doi.org/10.1103/PhysRevE.100.052601>
- [29] Sushko MYa (2007) Dielectric Permittivity of Suspensions. *J Exp Theor Phys* 105(2):426-431. <https://doi.org/10.1134/S1063776107080146>
- [30] Sushko MYa (2017) Effective dielectric response of dispersions of graded particles. *Phys Rev E* 96(6):062121(8 pages). <https://doi.org/10.1103/PhysRevE.96.062121>
- [31] Maxwell JC (1873) *A Treatise on Electricity and Magnetism*, Caledon Press, Oxford, vol. 1.
- [32] Rikvold PA, Stell G (1985) *D*-dimensional interpenetrable-sphere models of random two-phase media: Microstructure and an application to chromatography. *J Colloid Interface Sci* 108(1):158-173. [https://doi.org/10.1016/0021-9797\(85\)90246-2](https://doi.org/10.1016/0021-9797(85)90246-2)
- [33] Rikvold PA, Stell G (1985) Porosity and specific surface for interpenetrable-sphere models of two-phase random media. *J Chem Phys* 82:1014-1020. <https://doi.org/10.1063/1.448966>
- [34] Bikerman JJ (1940) Electrokinetic equations and surface conductance. A survey of the diffuse double layer theory of colloidal solutions. *Trans. Faraday Soc.* 35: 154-160. <https://doi.org/10.1039/TF9403500154>
- [35] Balika SD (2022) Determination of ζ -potential of nanofluids based on electrolyte solutions from the measurements by the methods of electrical spectroscopy and laser correlation spectroscopy. *Physics of Aerodisperse Systems* 60 (in press).
- [36] Balika SD and Sushko MYa (2022) Electrical conductivity of suspensions: Evidences for the stagnant layer contribution. *Ukrainian Conference with International Participation. Chemistry, Physics and Technology of Surface*.
- [37] Li L, Zhang Y, Ma H and Yang M (2010) Molecular dynamics simulation of effect of liquid layering around the nanoparticle on the enhanced thermal conductivity of nanofluids. *J. Nanopart. Res.* 12: 811-821. <https://doi.org/10.1007/s11051-009-9728-5>
- [38] Zhelezny V, Motovoy I, Khliyeva O and Lukianov N (2019) An influence of Al_2O_3 nanoparticles on the caloric properties and parameters of the phase transition of isopropyl alcohol in solid phase. *Thermochim Acta* 671: 170-180. <https://doi.org/10.1016/j.tca.2018.11.020>